Supporting Information for

Facile Fabrication of Nickel Oxide Nanostructures with High Surface Area and Application for Urease-based Biosensor for Urea Detection

Hien Duy Mai,[1] Gun Yong Sung,[2]* and Hyojong Yoo[1]*

[1]Department of Chemistry, Hallym University, Chuncheon, Gangwon-do, 200-702, Republic of Korea

[2]Department of Materials Science and Engineering, Hallym University, Chuncheon, Gangwon-do, 200-702, Republic of Korea

E-mail: hyojong@hallym.ac.kr (H. Yoo)

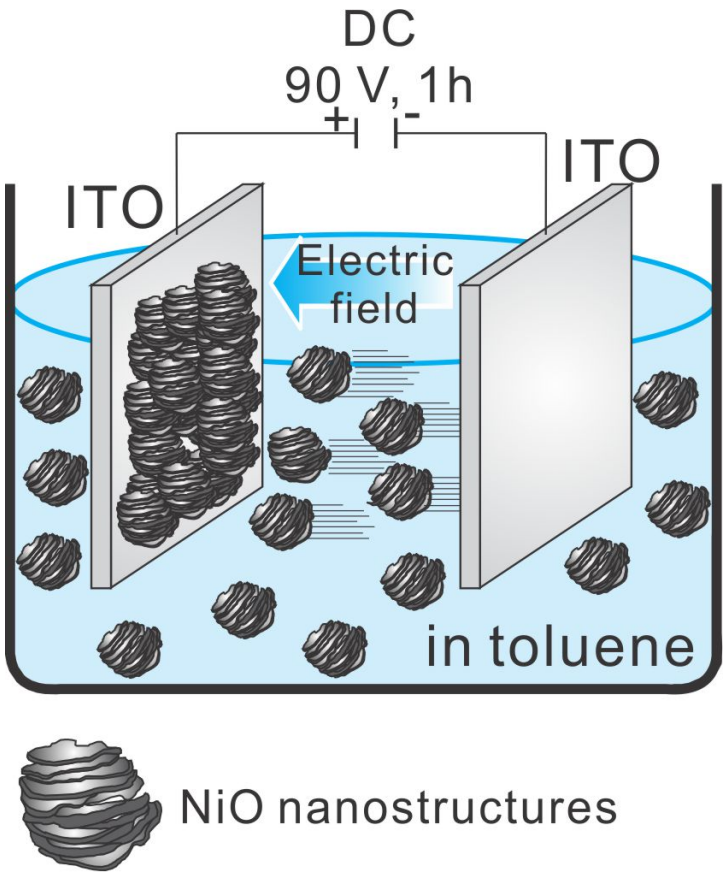

Fig. S1. Schematic diagram for the fabrication NiO/ITO electrodes through electrophoretic deposition (EPD) method.

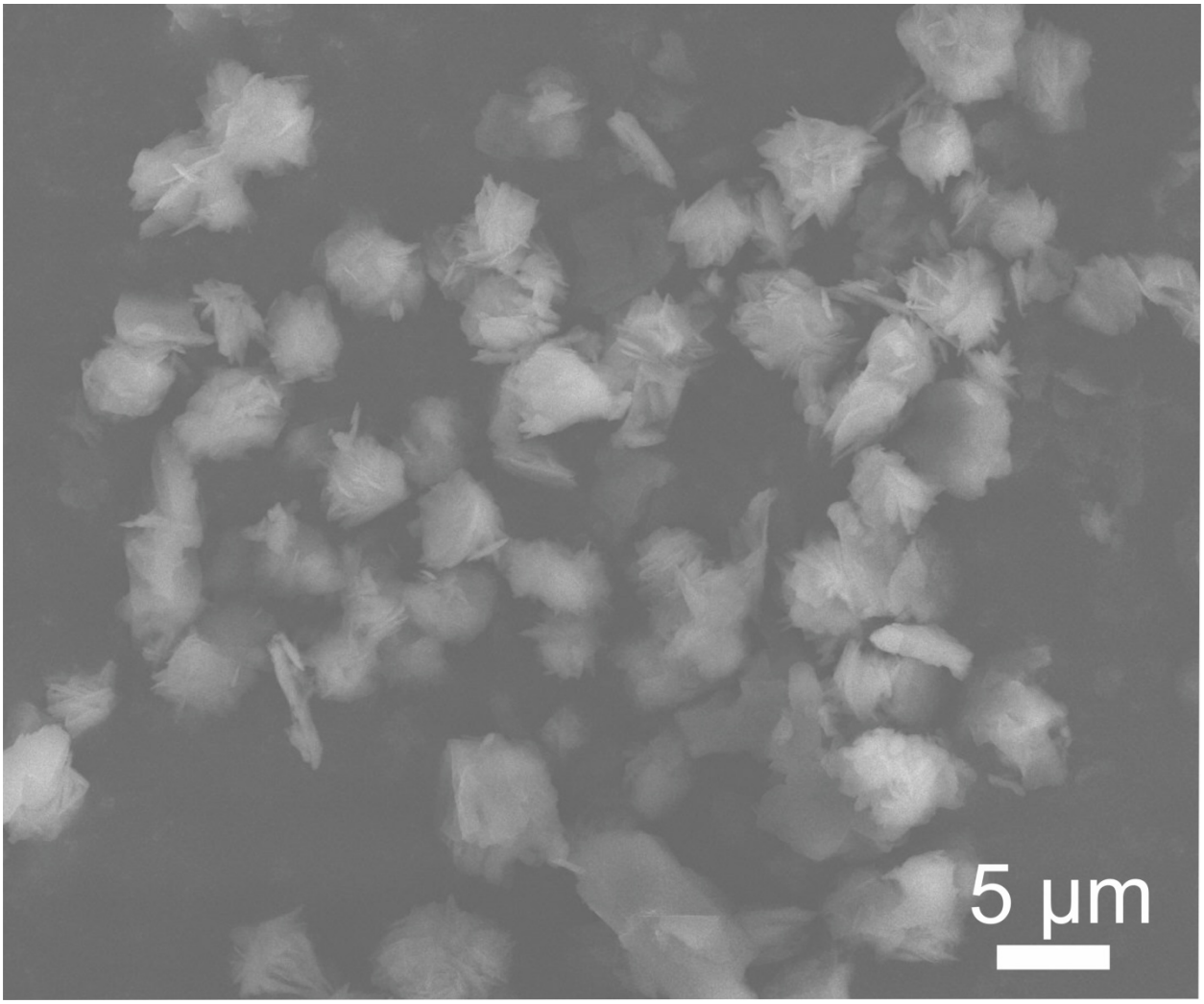

Fig. S2. SEM image of mL-NiCPPs.

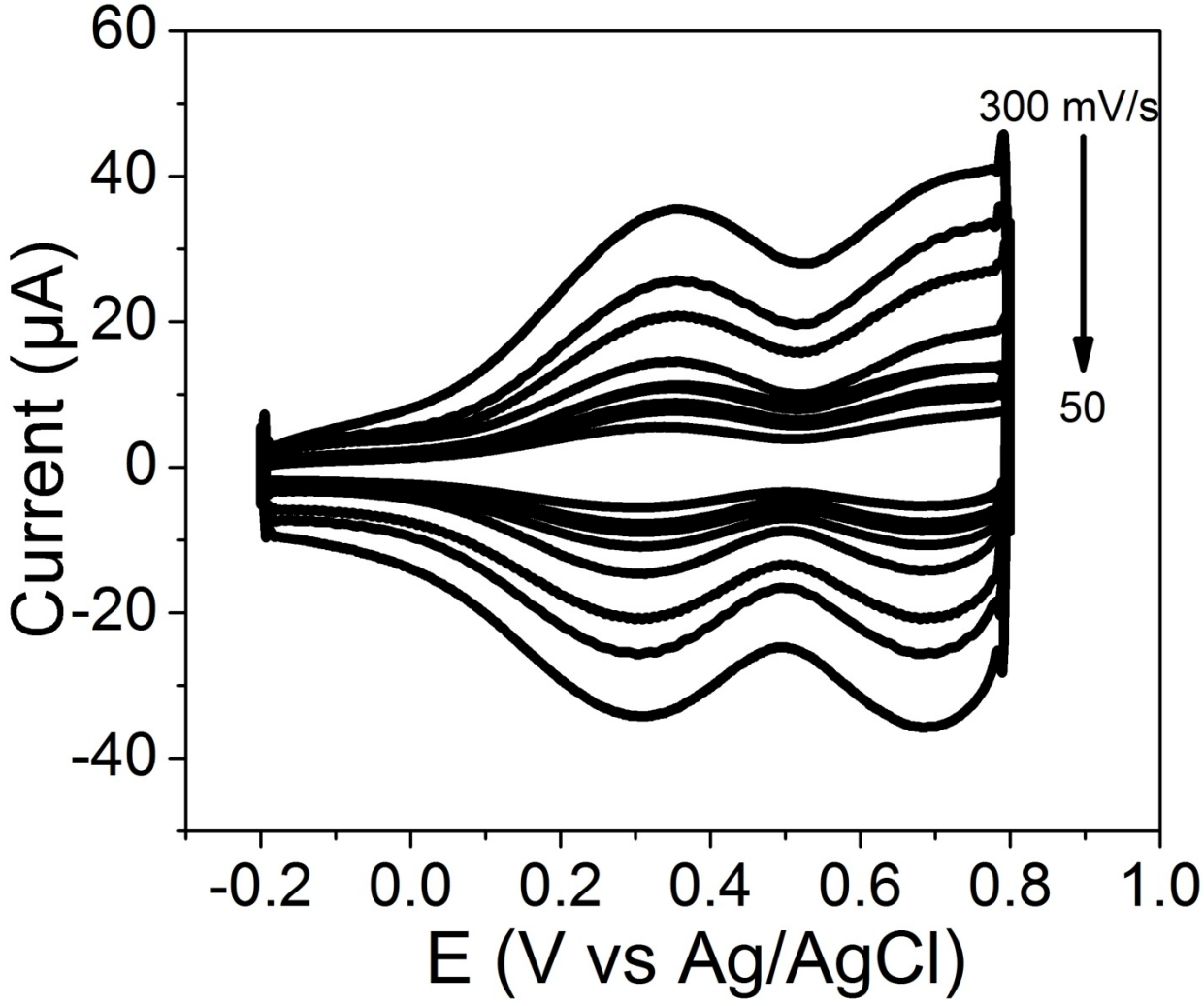

Fig. S3. Cyclic voltammograms (CVs) recorded at the NiO/ITO electrode prepared using dip coating method in a PBS buffer (10 mM; pH 7; NaCl $7\%_{ww}$) with different scan rate ranging from 50 to 300 mV/s.

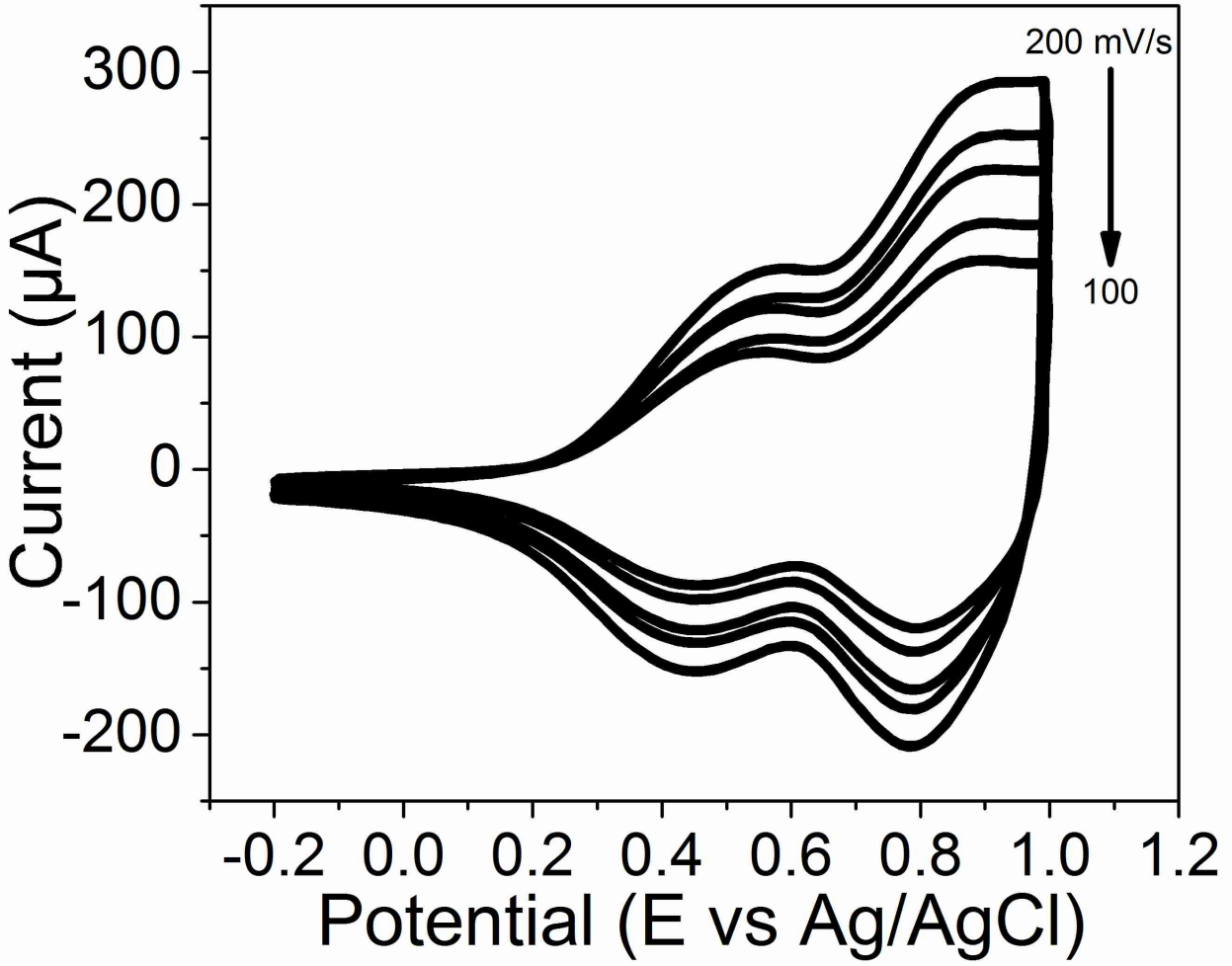

Fig. S4. Cyclic voltammograms (CVs) recorded at the NiO/ITO electrode prepared using EPD method in a PBS buffer (10 mM, pH 7; NaCl $7\%_{ww}$) with different scan rate ranging from 100 to 200 mV/s.

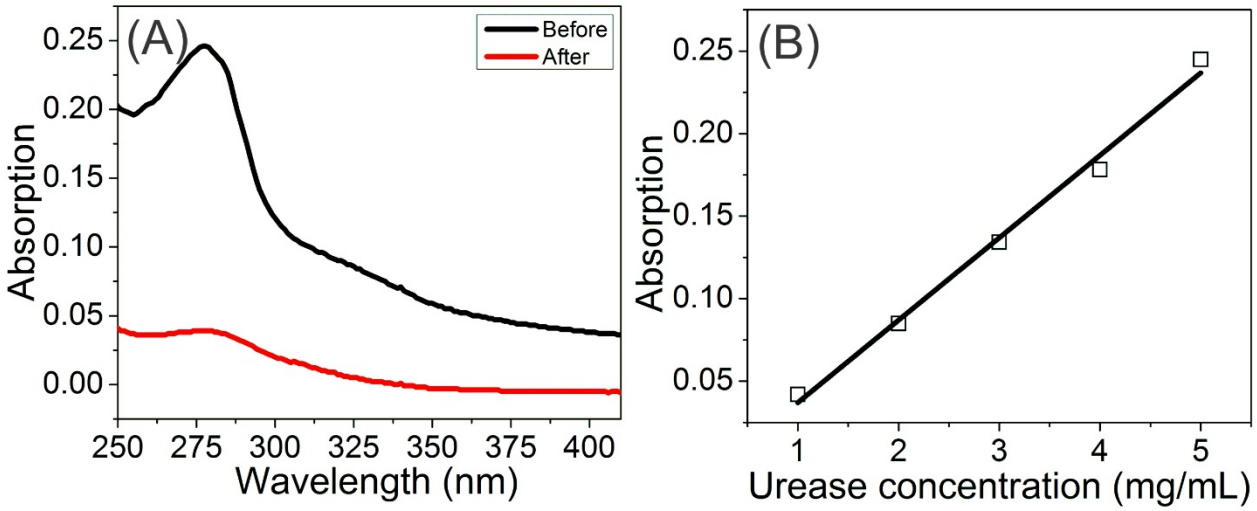

Fig. S5. (A) Ultraviolet-Visible (UV-Vis) spectra of urease solution (5 mg/mL, in PBS) before (black) and after (red) the immobilization step; (B) Calibration curve plotted between absorption peaks (at 278 nm) versus urease concentrations. Regression equation used to determine remaining urease concentration: Absorption intensity = 0.05*urease conc. – 0.01 (R^2 = 0.9907).

It is well known that UV-Vis spectrum of urease shows an absorption band with maximum peak at 278 nm,[9,10] which can be exploited to monitor concentration change of urease throughout the immobilization step. The amount of immobilized urease on the NiO/ITO electrode was determined as followings. Firstly, the UV-Vis spectrum of urease solution (5 mg/mL, in PBS) was recorded, showing strong absorption peak at 278 nm (Figure S5 A, black line). Two as-prepared NiO/ITO electrodes were then immersed into 2 mL of urease solution (5 mg/mL) for 2 hours at 25 ºC and this step was repeated 5 times. After the immobilization step, the UV-Vis spectrum of the urease solution was again recorded (Figure S5 A, red line). The remaining urease concentration estimated from the calibration curve (Figure S5 B) was 0.98 mg/mL. Therefore, the amount of immobilized urease on each NiO/ITO electrode was around 4.02 mg.

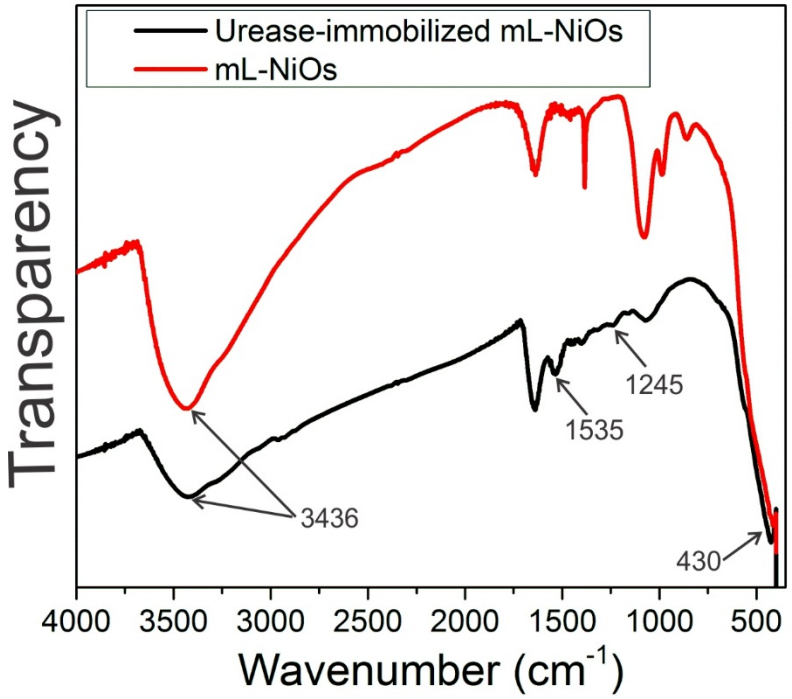

Fig. S6. FTIR spectra of mL-NiOs (red line) and urease-immobilized mL-NiOs (black line).

As observed in FTIR spectra of mL-NiOs and urease-immobilized mL-NiOs, two strong peaks at 430 and 3436 cm^{-1} are assigned to Ni-O vibration band.[11] More importantly, the successful immobilization of urease onto mL-NiOs was confirmed by emergence of urease characteristic peaks at 1535 and 1245 cm^{-1} corresponding to NH deformation mode and mixed vibration of C-N and N-H, respectively.[12]

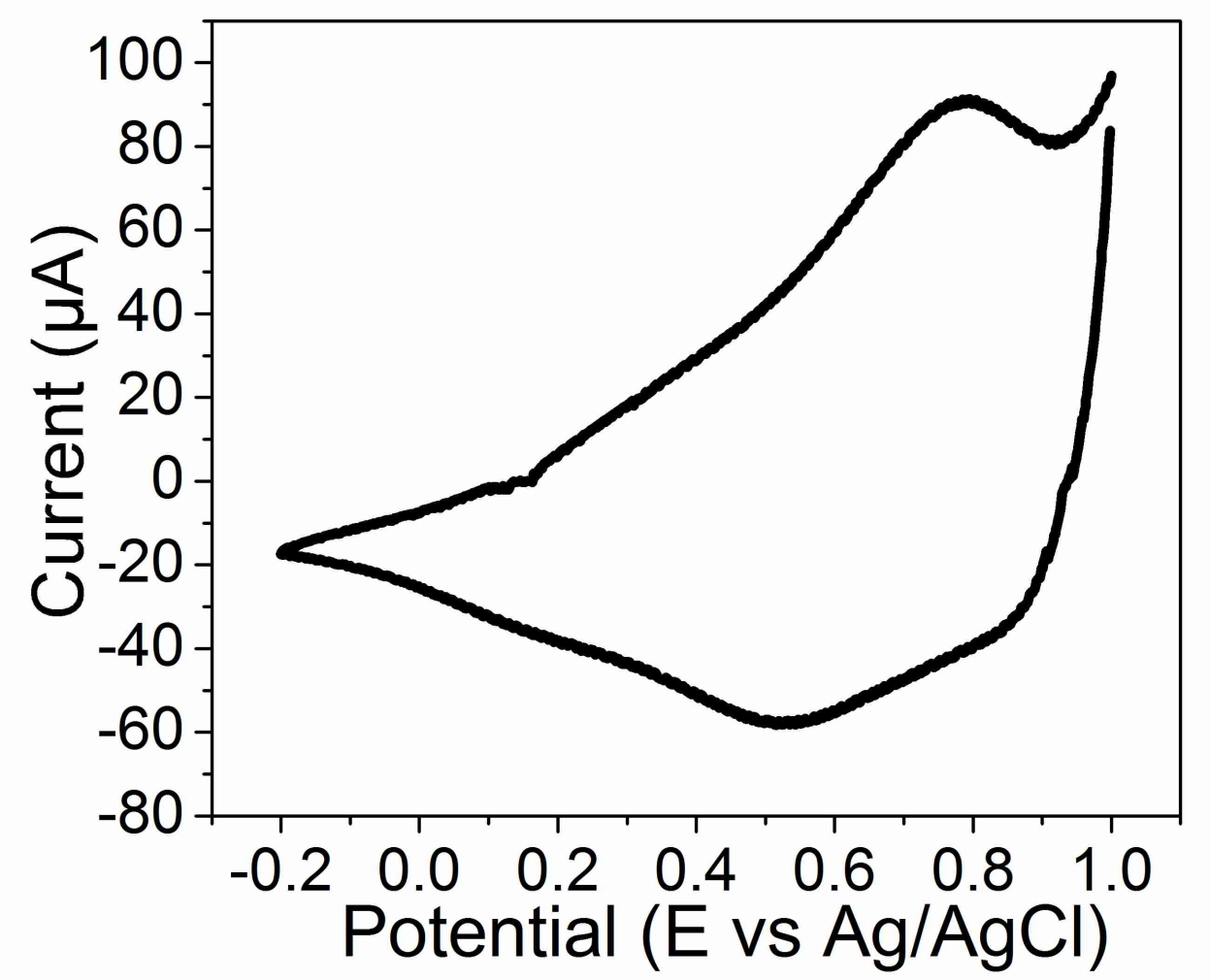

Fig. S7. Cyclic voltammogram recorded at the NiO/ITO electrode prepared in a PBS buffer (10 mM, pH 7; NaCl $7\%_{ww}$) showing no redox peaks corresponding to α-$Ni(OH)_2$/Ni couple arising at low potential (~ 0.4 V).

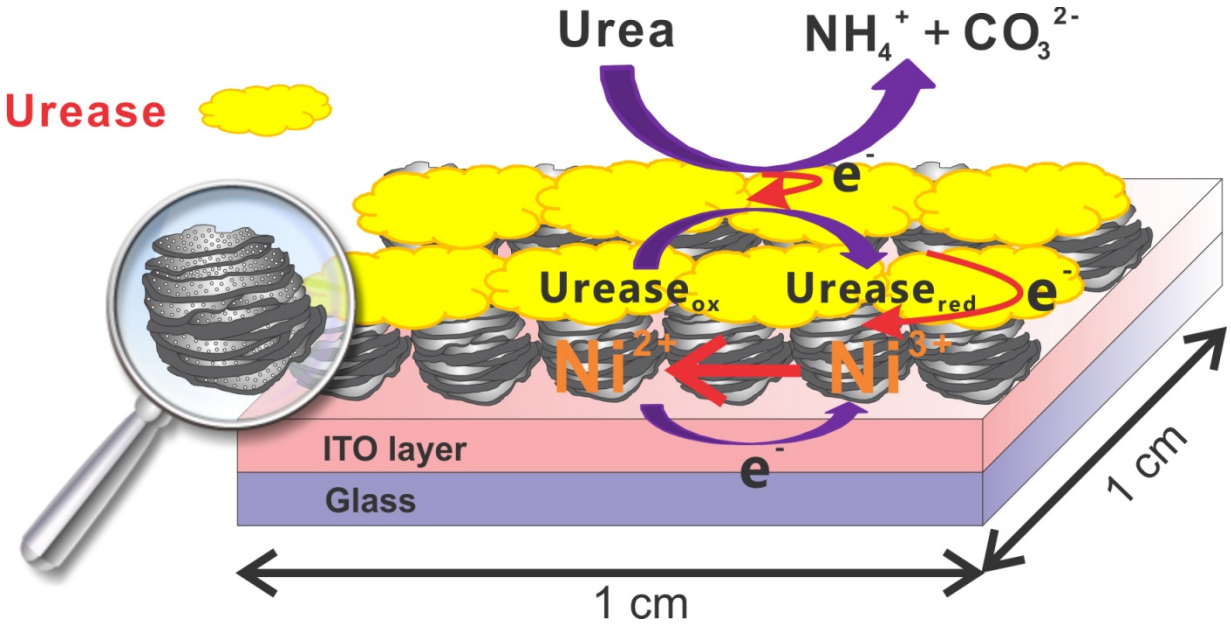

Fig. S8. Schematic diagram of the electrode reactions arising on the Ur-NiO/ITO electrode.

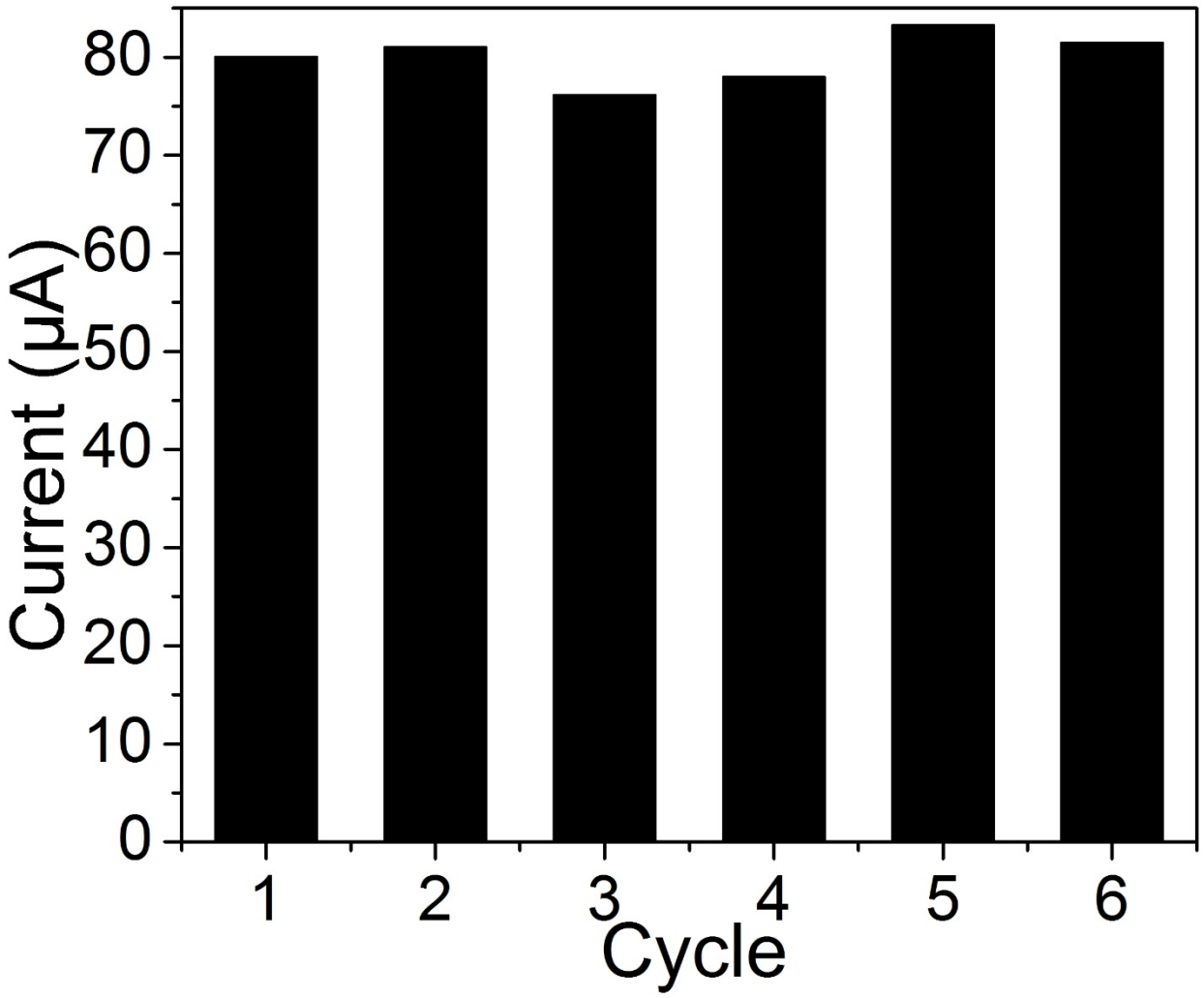

Fig. S9. Current measured in six repetitive cycles using the same Ur-NiO/ITO bioelectrode in the presence of 2 mM urea in PBS solution shows an accuracy of ± 6.58%.

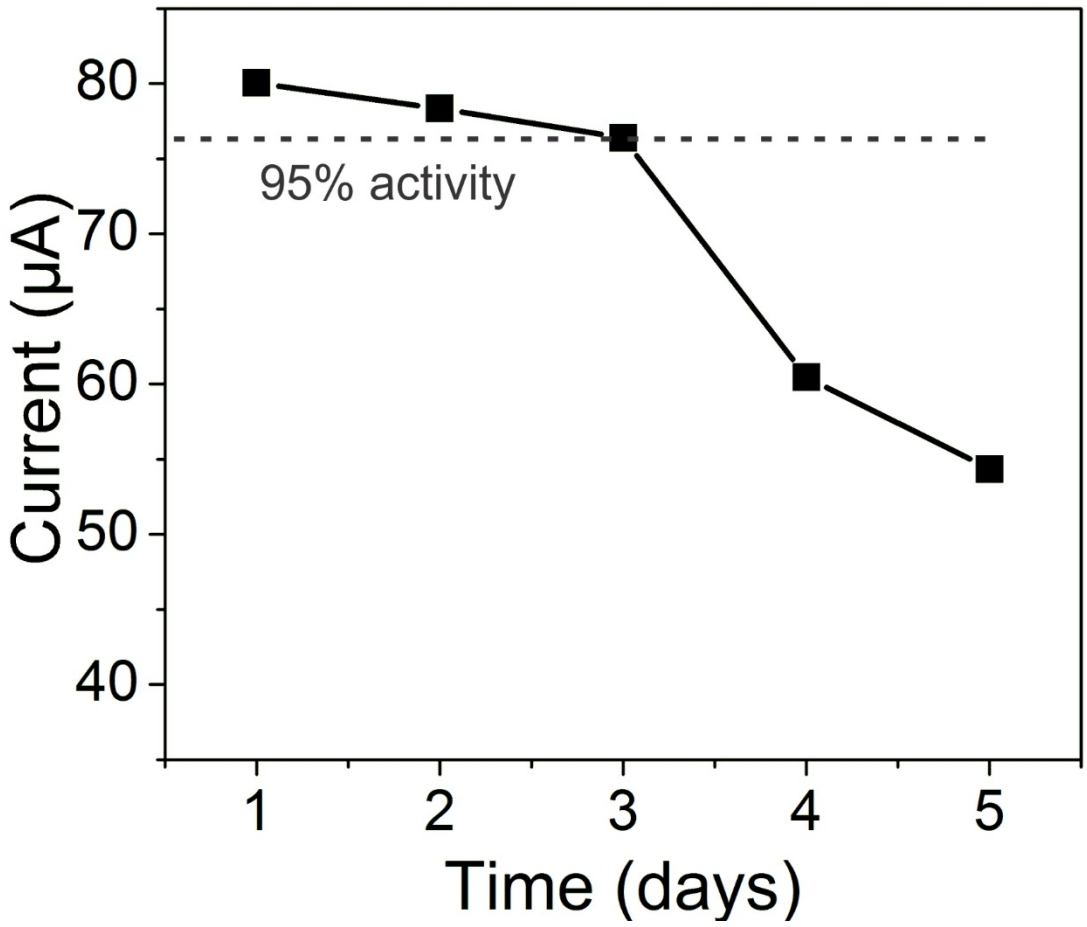

Fig. S10. The variation in the peak oxidation current of Ur-NiO/ITO bioelectrode over a period of five days, with a regular interval of one day. The bioelectrode maintained 95% of its activity throughout 3 days.

Table S1. Surface area values of the mL-NiOs and other NiO nanomaterials reported in the literature.

Samples	S_{BET} ($m^2 \cdot g^{-1}$)	Pore size (nm)	Pore volume ($cm^3 \cdot g^{-1}$)	Ref
NiO microspheres	130.2	5.0	0.163	1
NiO microspheres	113.3	5.4	0.209	1
NiO nanospindles	102.7	5-10		2
NiO nanoparticles	118	6	0.25	3
NiO nanoparticles	131.4	4	0.122	4
NiO nanosheets	194	3.5		5
NiO nanoparticles	88.5			6
NiO nanospheres	80.5	26		7
NiO nanoparticles	72.8	2.7-15		8
mL-NiOs	**112**	**10**	**0.4224**	Current work

* Those values are among the highest number for NiO nanoparticles that we have recorded thus far. Apart from that the reported surface area values of other NiO materials are much lower.

Reference and Notes

1. Pan, J. H.; Huang, Q.; Koh, Z. Y.; Neo, D.; Wang, X. Z.; Wang, Q. Scalable synthesis of urchin- and flowerlike hierarchical NiO microspheres and their electrochemical property for lithium storage. *ACS Appl. Mater. Interfaces* **2013**, *5*, 6292-6299.
2. Pang, H.; Zhang, B.; Du, J.; Chen, J.; Zhang, J.; Li, S. Porous nickel oxdie nanospindles with huge specific capacitance and long-life cycle. *RSC Adv.* **2012**, *2*, 2257-2261.
3. Meng, T.; Ma, P.- P.; Chang, J.- L.; Wang, Z.- H.; Ren, T.- Z. The electrochemical capacitive behaviors of NiO nanoparticles. *Electrochim. Acta* **2014**, *125*, 586-592.
4. Kalam, A.; Al-Shihri, A. S.; Al-Sehemi, A. G.; Awwad, N. S.; Du, G.; Ahmad, T. Effect of pH on solvothermal synthesis of (beta)-Ni(OH)2 and NiO nanoarchitectures: Surface area studies, optical properties and adsorption studies. *Superlattice. Microst.* **2013**, *55*, 83-97.
5. Hoa, N. D.; El-Safty, S. A. Synthesis of mesoporous NiO nanosheets for the detection of toxic NO_2 gas. *Chem.- Eur. J.* **2011**, *17*, 12896-12901.
6. Farhadi, S.; Kazem, M.; Siadatnasab, F. NiO nanoparticles prepared via thermal decomposition of the bis(dimethylglycoximato)nickel (II) complex: a novel reusable heterogeneous catalyst for fast and efficient microwave-assisted reduction of nitroarenes with ethanol. *Polyhedron,* **2011***, 30,* 606-613.
7. Zhang, G.; Chen, Y.; Qu, B.; Hu, L.; Mei, L.; Lei, D.; Li, Q.; Chen, L.; Li, Q.; Wang, T. Synthesis of mesoporous NiO nanospheres as anode materials for lithium ion batteries. *Electrochim. Acta.* **2012**, *80*, 140-147.
8. Gu, C. D.; Huang, M. L.; Ge, X.; Zheng, H.; Wang, X. L.; Tu, J. P. NiO electrode for methanol electro-oxidation: mesoporous vs. nanoparticulate. *Int. J. Hydrogen. Energ.* **2014**, *39*, 10892-10901.
9. Wang, Y.-Q.; Zhang, G.-C.; Zhang, H.-M. Study on the Interaction of Pentachlorophenol with Urease in Aqueous Solution by Multiple Spectroscopic Techniques. *J. Solution Chem.* **2011**, *40*, 458-469.

10. Wang, Y.-Q.; Zhang, H.-M. Spectral studies on the interaction between Cu^{2+} and urease. *Spectrochimica Acta Part A: Molecular and Biomolecular Spectroscopy* **2012**, *96*, 352-357.
11. Su, D.; Kim, H.-S.; Kim, W.-S.; Wang, G. Mesoporous Nickel Oxide Nanowires: Hydrothermal Synthesis, Characterisation and Applications for Lithium-Ion Batteries and Supercapacitors with Superior Performance. *Chem. Eur. J.* **2012**, *18*, 8224-8229.
12. Ogura, K.; Nakaoka, K.; Nakayama, M.; Kobayashi, M.; Fujii, A. *Analytica Chimica Acta* **1999**, *384*, 219-225.